



Clinical report

Severe ipsilateral musculoskeletal involvement in a Cornelia de Lange patient with a novel *NIPBL* mutation



Carolina Baquero-Montoya^{a,c}, María-Concepción Gil-Rodríguez^a,
 María Hernández-Marcos^a, María-Esperanza Teresa-Rodrigo^a, Alicia Vicente-Gabas^{a,b},
 María-Luisa Bernal^a, Cesar-Horacio Casale^d, Gloria Bueno-Lozano^b,
 Inés Bueno-Martínez^{a,b}, Ethel Queralt^e, Olaya Villa^f, Cristina Hernando-Davalillo^f,
 Lluís Armengol^f, Paulino Gómez-Puertas^g, Beatriz Puisac^a, Angelo Selicorni^h,
 Feliciano J. Ramos^{a,b}, Juan Pié^{a,*}

^a Unit of Clinical Genetics and Functional Genomics, Departments of Pharmacology- Physiology and Pediatrics, Medical School, University of Zaragoza, Spain

^b Service of Pediatrics, Hospital Clínico Universitario "Lozano Blesa", Zaragoza, Spain

^c Department of Pediatrics, Hospital Pablo Tobón Uribe, Medellín, Colombia

^d Department of Molecular Biology, Sciences School, National University of Río Cuarto, Argentina

^e Cell Cycle Group, Cancer Epigenetics and Biology Program (PEBC), Institut d'Investigacions Biomèdica de Bellvitge (IDIBELL), L'Hospitalet de Llobregat, Barcelona, Spain

^f Quantitative Genomic Medicine Laboratories, Barcelona, Spain

^g Molecular Modelling Group, Center of Molecular Biology "Severo Ochoa" (CSIC-UAM), Cantoblanco, Madrid, Spain

^h Pediatric Clinic, University of Milano Bicocca, San Gerardo Hospital, Monza, Italy

ARTICLE INFO

Article history:

Received 26 September 2013

Accepted 14 May 2014

Available online 27 May 2014

Keywords:

Cornelia de Lange Syndrome
 CdLS

HEAT repeat

Ipsilateral

Musculoskeletal involvement

NIPBL mutation

BHLHA9 duplication

Exome sequencing

ABSTRACT

Cornelia de Lange Syndrome (CdLS) is a congenital autosomal dominant (*NIPBL*, *SMC3* and *RAD21*) or X-linked (*SMC1A* and *HDAC8*) disorder characterized by facial dysmorphism, pre and postnatal growth retardation, developmental delay and/or intellectual disability, and multiorgan involvement. Musculoskeletal malformations are usually bilateral and affect mainly the upper limbs; the range goes from brachyclinodactyly to severe reduction defects. Instead lower extremities are usually less and mildly involved. Here, we report on a 3-year-old Senegalese boy with typical craniofacial CdLS features, pre and postnatal growth retardation, atrial septal defect, developmental delay and right ipsilateral limb malformations, consistent with oligodactyly of the 3rd and 4th fingers, tibial agenesis and fibula hypoplasia. Exome sequencing and Sanger sequencing showed a novel missense mutation in *NIPBL* gene (c.6647A>G; p.(Tyr2216Cys)), which affects a conserved residue located within *NIPBL* HEAT repeat elements. Pyrosequencing analysis of *NIPBL* gene, disclosed similar levels of wild-type and mutated alleles in DNA and RNA samples from all tissues analyzed (oral mucosa epithelial cells, peripheral blood leukocytes and fibroblasts). These findings indicated the absence of somatic mosaicism, despite of the segmental asymmetry of the limbs, and confirmed biallelic expression for *NIPBL* transcripts, respectively. Additionally, conditions like Split-hand/foot malformation with long-bone deficiency secondary to duplication of *BHLHA9* gene have been ruled out by the array-CGH and MLPA analysis. To our knowledge, this is the first CdLS patient described with major ipsilateral malformations of both the upper and lower extremities, that even though this finding could be due to a random event, expands the spectrum of limb reduction defects in CdLS.

© 2014 Elsevier Masson SAS. All rights reserved.

* Corresponding author. Unit of Clinical Genetics and Functional Genomics, Department of Pharmacology and Physiology, University of Zaragoza, Medical School, c/Domingo Miral s/n, Zaragoza E-50009, Spain. Tel.: +34 976 76 16 77; fax: +34 976 76 17 00.

E-mail address: juanpie@unizar.es (J. Pié).

1. Introduction

Mutations in components of the cohesin complex (*SMC1A*, *SMC3* and *RAD21*) and its regulatory proteins (*NIPBL* and *HDAC8*) are responsible for Cornelia de Lange Syndrome (CdLS). Indeed, heterozygous mutations in *NIPBL* gene, which codifies the human

ortholog of the *Drosophila* Nipped-B and yeast Scc2 proteins, were the first demonstrated cause of CdLS (CDLS1, OMIM 122470) and account for ~70% of cases with classical phenotype [Deardorff et al., 2007, 2012a, 2012b; Krantz et al., 2004; Musio et al., 2006; Selicorni et al., 2007; Tonkin et al., 2004]. NIPBL facilitates cohesin loading on chromatin, while the cohesin complex mediates the sister chromatid cohesion, DNA reparation, gene regulation and maintenance of genome stability, among other functions [Liu and Krantz, 2009].

CdLS is a congenital developmental disorder characterized by a broad spectrum of clinical findings, like typical facial features, pre and postnatal growth retardation, developmental delay and/or intellectual disability, and a wide range of limb abnormalities [Kline et al., 2007]. In the upper limbs the malformations can vary from small hands with 5th finger clinodactyly, to oligodactyly, ulnar deficiency and absent forearm [Kline et al., 2007]. The lower extremities usually are less involved, generally with mild anomalies such as clubbed foot deformity and/or partial 2nd and 3rd toes syndactyly [Kline et al., 2007; Roposch et al., 2004].

Here, we describe the clinical and molecular characteristics of the first reported case with a novel missense NIPBL mutation (c.6647A>G, p.(Tyr2216Cys)), which results in a classic CdLS phenotype. The clinical finding of a severe ipsilateral involvement of the right upper and lower extremities, suggests the coexistence of CdLS with the Tibial Aplasia-Ectrodactyly Syndrome or perhaps other congenital limb malformation. The possibility of the presence of both conditions as well as the possibility of somatic mosaicism has been rule out by exome sequencing, Sanger sequencing, aCGH, MLPA and pyrosequencing DNA samples from different tissues. Additionally the mutated allele expression has been confirmed. Further bioinformatic analysis of structural position and conservation of mutated residue within the HEAT repeat domain of NIPBL has also been performed.

2. Clinical report

The patient is the second child of consanguineous Senegalese parents aged 44 and 29 years at the time of conception. During the

first trimester of gestation, a possible congenital heart malformation was detected in the prenatal ultrasound (US). He was born at 39 weeks by vaginal delivery. Apgar score was 9 in the first minute and 10 at 5 min. Birth weight was 2230 gr, length 44.5 cm and head circumference (HC) 31 cm (<3rd centile for gestational age). In the newborn period, the craniofacial features included synophrys with arched eyebrows, long eyelashes, depressed nasal bridge with antverted nostrils, low set ears, long and prominent philtrum, thin lips with down-turned corners, high arched palate, micrognathia, low anterior and posterior hairline, generalized hirsutism and *cutis marmorata* (Fig. 1 a). He had oligodactyly of the 3rd and 4th fingers (Fig. 1 d-e and f-g). In the right limb he had distal hypoplasia that caused foot deformity (Fig. 1 b). Roentgenographic studies of that leg showed tibial agenesis and fibular hypoplasia (Fig. 1 c). The left limbs were apparently normal (Fig. 1 b and c). The echocardiogram showed an atrial septal defect (which spontaneously resolved at 2 years of age). During the first months of life, he had a feeding and swallowing disorder. Barium contrast radiography did not show spontaneous gastroesophageal reflux. At the age of 1 year, he was surgically intervened for the amputation of the right leg.

At the last examination, at the age of 4 years, his weight was 13.6 Kg (7th centile), his height was 90.7 cm and his HC was 47 cm (both <3rd centile). Developmental milestones were delayed. He was able to sit unsupported at the age of 6 months and to walk with lower limb prosthesis, at 3 years old. He only says 3–4 words.

3. Methods

3.1. Genomic DNA and RNA extraction

We collected DNA and RNA samples from tissues with different and/or similar embryological origin (ectoderm (oral mucosa epithelial cells) and/or mesoderm (peripheral blood leukocytes and fibroblasts)). Genomic DNA was extracted from peripheral blood leukocytes and cultured skin fibroblasts by standard procedures. By contrast, RNA was extracted from blood leukocytes by the PAXgene



Fig. 1. Phenotype of the patient. (a–b) Frontal view and lower limbs of the patient in the first week of life; (c) Roentgenogram of the lower extremities at three years of age; (d–e) Right and left hands and (f–g) Roentgenogram of the right and left hands at three years of age.

Blood RNA Kit (PreAnalytiX) according the manufacturer's instruction, as well as RNA from the cultured fibroblasts, it was isolated using the RNeasy Protect Mini Kit (QIAGEN). The Oragene DNA Self-Collection kit (DNAgenotek®) was used to collect and extract DNA from saliva.

3.2. Exome sequencing

Briefly, 1 µg of genomic DNA in 100 µL volume was sheared into fragments of approximately 300 base pairs using Covaris instrument. Genomic DNA samples were constructed into Illumina Pair-End pre-capture libraries according to the manufacturer's protocol. Pre-capture library (1 µg) was hybridized in solution to the Sure-Select Human All Exon V5+UTRs exome capture platform (Agilent) according to the manufacturer's protocol. This exome kit version targets coding regions plus UTRs. Library templates were prepared for sequencing using Illumina's cBot cluster generation system with the corresponding TruSeq PE Cluster Kits for the HiSeq 2000. An average per-base coverage >75× was achieved. Exome data was analyzed using standard procedures: Alignment with BWA, refinement with picard and samtools, variant calling with GATK, annotation of relevant information with ANNOVAR and own scripts.

3.3. Molecular testing by Sanger sequencing

Screening for mutations was performed on DNA from blood leukocytes by PCR amplification of the exons 2–47 of the *NIPBL* gene and its intron–exon boundaries, and by bidirectional direct sequencing. Reference sequence used for *NIPBL* was NM_133433.3. The nucleotide position of variants reflects cDNA numbering with +1 corresponding to the A of the ATG translation initiation codon.

3.4. Array comparative genomic hybridization (aCGH)

Microarray analysis was performed using a commercially available CGH microarray from Agilent Technologies (Santa Clara, CA). The slide contains nearly 1 million oligonucleotide probes scattered throughout the genome, with a 3 Kb overall median probe spacing, according to the manufacturer. After hybridization and washings, slide was scanned and analyzed for relative gain or loss of fluorescent signals from hybridization of the proband vs reference DNAs. The detection of copy number variations was performed on the Genomic Workbench software (v 5.0), using ADM-2 algorithm, with a minimum of 6 consecutive oligonucleotides probes exceeding an absolute \log_2 ratio threshold of 0.25 (thus with a practical resolution of 18 Kb). Genomic positions were referred to NCBI's human sequence build 36.1 (hg18).

3.5. Multiplex ligation-dependent probe amplification (MLPA)

A total of 150 ng of genomic DNA from the patient's sample and 14 controls was subject to MLPA using specific synthetic probes designed to target the *BHLHA9* gene and its regulatory region. The MLPA reactions were performed as described previously and products were analyzed on an ABI PRISM 3100 Genetic Analyzer according to manufacturer's instructions. For quantitative analysis, trace data were retrieved using the accompanying software (GeneScan, Applied Biosystems). Each MLPA signal was normalized and compared with the corresponding mean peak height obtained from fifteen control DNA samples.

3.6. Quantitative mutational analysis by pyrosequencing

To explore the possibility of a somatic mosaic mutation, we tested the presence of the c.6674A>G mutation in DNA from tissues

with different and/or similar embryological origins by pyrosequencing quantitative assay. Biotinylated and normal primers targeting exon 39 of the *NIPBL* gene were used for amplification. Subsequent to capture of PCR products on Streptavidin Sepharose HP (GE Healthcare), single-stranded DNA separation and hybridization of sequencing primer, pyrosequencing was carried out on a PSQ™ 96 MA system (Qiagen). The resulting data were analyzed and quantified with the PSQ™ 96 MA 2.1 software (Qiagen) and validated by Sanger sequencing.

3.7. RT-PCR and allele-specific expression analyses

Subsequently, we quantified allele specific expression for *NIPBL* transcripts in different mesoderm's tissues using pyrosequencing. First, RT-PCR reactions were performed using the First Strand Synthesis Kit (Fermentas) with random hexamers, according to the manufacturer's protocol. Pyrosequencing reaction was performed as previously described.

3.8. Bioinformatic analysis

The pathological significance of the variants was initially tested with PolyPhen-2 (<http://genetics.bwh.harvard.edu/pph/>) and SIFT (<http://sift.jcvi.org/>) online software. In order to analyze in detail the putative structural implication of the mutation, a three-dimensional structural model for the HEAT-repeat region of human *NIPBL* (residues 1760–2349) was generated using homology modeling procedures and automated methods developed by Biomol-Informatics SL ([Supporting information online](#)).

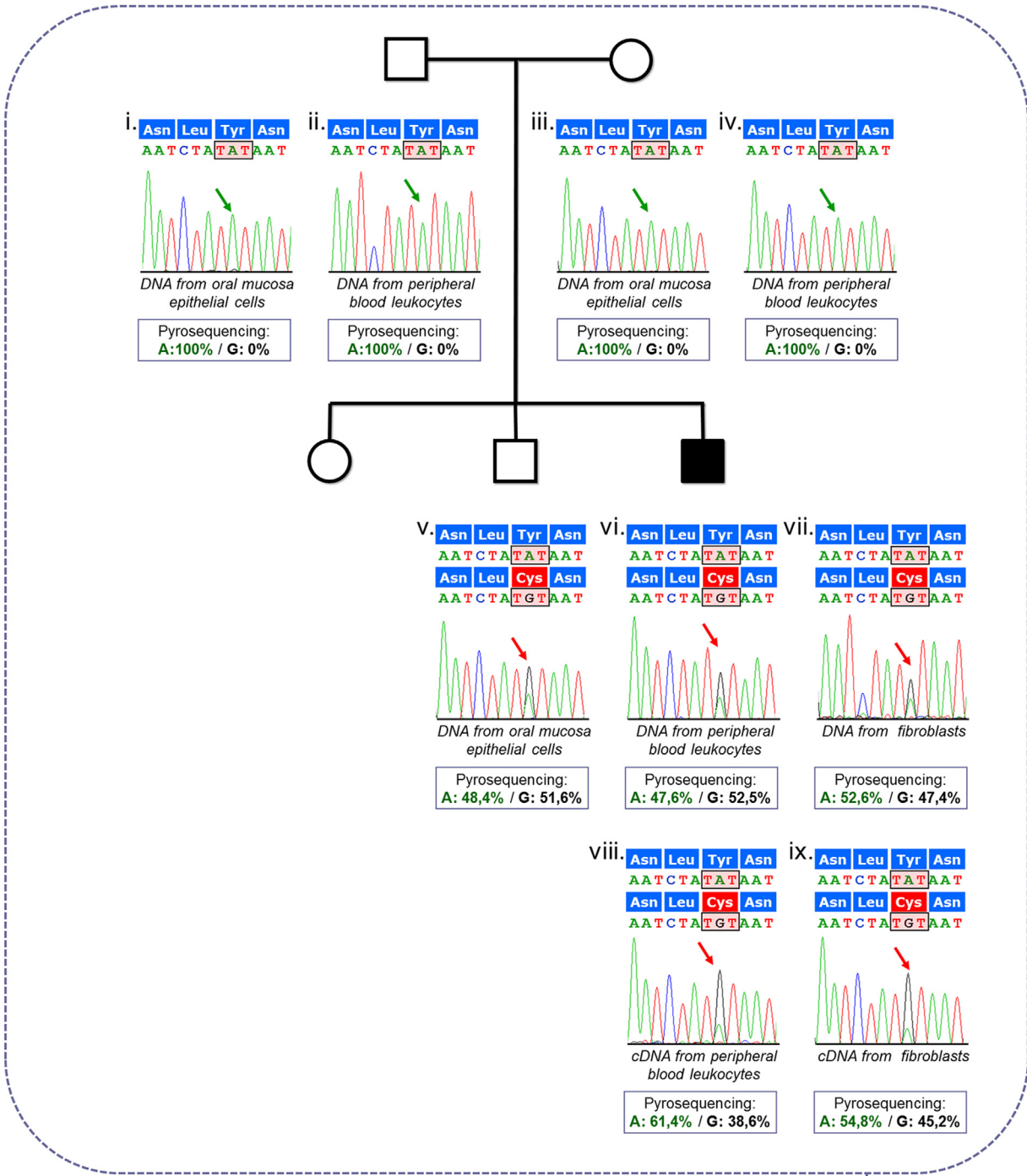
4. Results

Exome sequencing and Sanger sequencing analyses of the patient's DNA only demonstrated heterozygosity for A>G change at position 6647 of the *NIPBL* gene (Fig. 2a_v–vii) (Supplementary Tables 1–4). However, an additional list of all variants identified in this patient's exome that might be relevant to check under different hypothesis of inheritance models (Supplementary Tables 1–4) is provided. Besides, pyrosequencing results confirmed this genotype and showed that the mutation was present in a similar wild-type allele percentage in the total sequence tested, with a mean of $51.6\% \pm 1.1\%$, $52.5\% \pm 0.5\%$ and $47.4\% \pm 1.0\%$ in oral mucosa epithelial cells, peripheral blood leukocytes and fibroblast respectively (Fig. 2a_v–vii). Analysis of the available parental samples revealed only the normal allele (Fig. 2a_i–iv), suggesting a *de novo* event.

We confirmed biallelic expression, as well as quantified allele-specific expression for *NIPBL*, in different tissues using pyrosequencing too (Fig. 2a_viii–ix). We determined that, in patient peripheral blood cells, the mutant allele contributed only to $38.6\% \pm 1.1\%$, while in fibroblast, was present in $45.2\% \pm 1.1\%$. These results were also validated by traditional sequencing as previously described (Fig. 2a_viii–ix).

The c.6647A>G mutation leads to amino acid substitution of one residue highly conserved during evolution, p.(Tyr2216Cys), as the protein alignment from different species predicts (Fig. 3b). Its effect on *NIPBL* protein was predicted as damaging according to online programs. In the obtained structural model (Fig. 3a, top), position of Tyrosine 2216 was predicted to be located in an alpha-helix, positioned in an internal location in close contact to residues Leu2196, Phe2208 and Val2212 (Fig. 3a_i, bottom left), participating in the structural stability of the local sub-domain. Substitution of Tyr 2216 by Cys in the *NIPBL* protein (Fig. 3a_ii, bottom right) will disturb the close contacts, generating a local disorganization of the protein folding which could result in its inactivation.

(a)



(b)

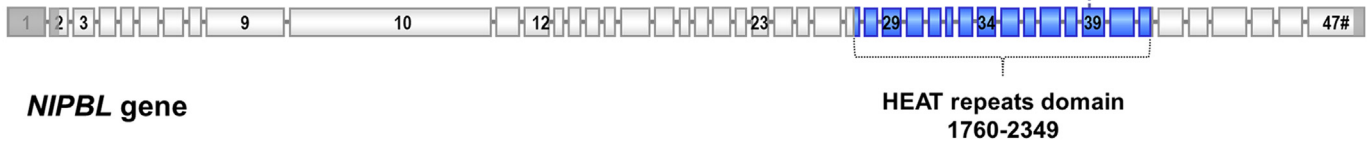


Fig. 2. (a) Pedigree of the proband, partial electropherograms of the exon 39 of NIPBL and pyrosequencing results. The traditional sequencing analysis performed on genomic DNA from the patient oral mucosa epithelial cells, peripheral blood leukocytes and fibroblasts (v–viii), as well as cDNA from blood leukocytes and fibroblasts (viii–ix) shows the peaks of

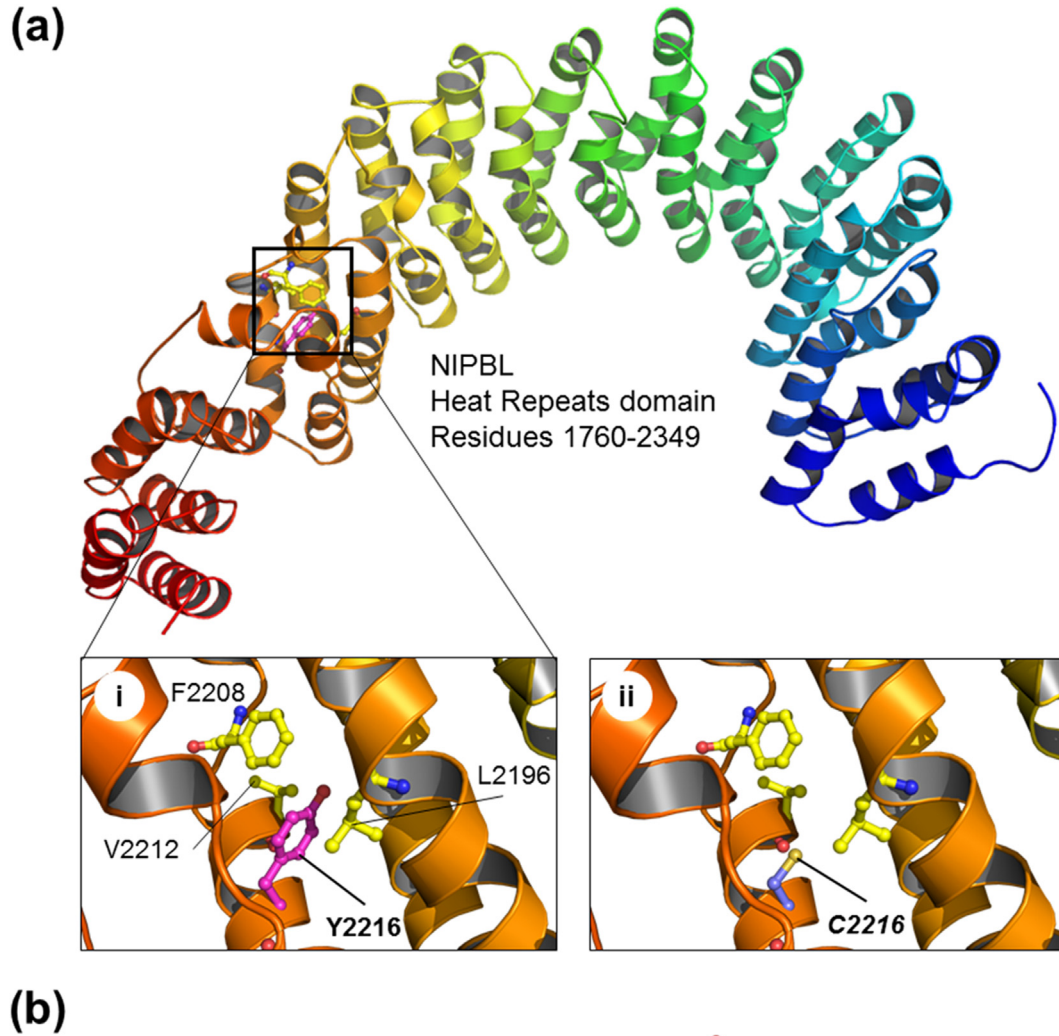


Fig. 3. Bioinformatic analysis and 3-D modeling of the predicted HEAT repeat domain of NIPBL. (a) Position of wild-type amino acid (Y2216) and mutated residue (C2216) in the proposed structural model for HEAT domain of NIPBL protein (residues 1760–2349). Figures were generated using the Pymol Molecular Graphics System (Schrödinger, LLC). (b) Multiple sequence alignment of NIPBL to several organisms in the area surrounding mutated residue Y2216 (labeled with a red dot in the alignment). Represented NIPBL sequences are from: *Homo sapiens* (Human), *Mus musculus* (Mouse), *Rattus norvegicus* (Rat), *Equus caballus* (Horse), *Oryctolagus cuniculus* (Rabbit), *Gallus gallus* (Chick), *Xenopus laevis* (Xenopus), *Drosophila melanogaster* (Drosophila) and *Caenorhabditis elegans* (C. Elegans).

The presence of copy number alterations in the *BHLHA9* locus was ruled out by MLPA and chromosomal microarray-based analysis. In addition, aCGH also allowed to discard the presence of any other relevant pathogenic copy number variant in this patient. Finally, no relevant variants were found in the exons of the causal genes of other musculoskeletal malformations analyzed by exome sequencing (Supplementary Table 2).

5. Discussion

Here, we described a CdLS proband, who has ipsilateral oligodactyly, tibial agenesis with fibular hypoplasia and carries a novel missense mutation in exon 39 of the *NIPBL* gene, c.6647A>G, detected by Exome sequencing (Supplementary Tables 1–4) and Sanger sequencing approaches.

The association between CdLS and musculoskeletal malformations is well known [Kline et al., 2007]. The upper extremities are typically involved with a variety of anomalies ranging from small hands, shortening of the first metacarpal with proximally placed thumbs, brachydactyly, 5th finger clinodactyly and single palmar crease to hypoplasia of the proximal radial head, ulnar deficiency, oligodactyly/ectrodactyly and absent arm [Kline et al., 2007]. Anomalies of lower limbs are uncommon and milder, and include being small feet, 2nd – 3rd toes syndactyly, bilateral hallux valgus, short 3rd and 4th metatarsal bones and bilateral equinovarus feet [Bhuiyan et al., 2006; Kline et al., 2007]. Nevertheless, lower limb reduction defects have been occasionally described in CdLS individuals [Kline et al., 2007]. In addition, the simultaneous association of severe reduction defects of upper and lower extremities has not been reported so far in CdLS, and, as far as we know, our proband is the first reported case this striking involvement.

Lower musculoskeletal involvement is a common clinical finding in other cohesinopathies like Roberts- SC Phocomelia syndrome, in which hypomelia, tetrachomelia, absence or reduction in length of the upper and/or lower extremities can be seen [Ahmed et al., 2009]. However, in CdLS severe reduction defects of the lower extremities are infrequent, and the reported cases included bilateral hypoplasia or aplasia of the tibia and/or the fibula and more rarely bifurcated femur [Kline et al., 2007; Pfeiffer and Correll, 1993]. Interestingly, segmental body asymmetry or ipsilateral association of oligodactyly with tibial agenesis and fibula hypoplasia have not been disclosed in CdLS.

Among conditions, which showed this type of unusual congenital limb malformations, the Tibial Aplasia-Ectrodactyly syndrome must be highlight. In order to rule out the coexistence of both syndromes, the assessment of the roentgenograms of the left limbs and the analysis of copy number variations in the *BHLHA9* locus by MLPA and aCGH have been performed, since only genomic duplications encompassing this gene have been reported [Petit et al., 2013]. Furthermore, taking into account the familial background of consanguinity, an exome sequencing approach was carried out. Despite of a careful analysis of the reported causative genes of congenital musculoskeletal malformations, no relevant variants were found (Supplementary Tables 1–4). Considering these data all together, we suggest that the mutation in *NIPBL* may be the cause of the ipsilateral musculoskeletal involvement in this subject, but always keeping in mind that these finding might be due to a random event. The recent report of two cases of CdLS with bilateral split foot along with our case, clearly expands the spectrum of the lower limb malformations in CdLS [Barboni et al., 2012; Dogan et al., 2010].

Most often, extremities reduction defects indicate the presence of a severe clinical involvement and a worse prognosis [Gillis et al., 2004]. In our proband, even in the context of a segmental body asymmetry, it was noteworthy the absence of other major anomalies and the mild cognitive impairment. It is well known that segmental body asymmetry is an important clue for somatic mosaicism, [Yousoufian and Pyeritz, 2002] which added to the recent description of 10 mosaic-*NIPBL* CdLS probands [Huisman et al., 2013], prompted us to perform molecular analyses in several body tissue samples from different embryological origins. The pyrosequencing studies in our patient revealed an equal level of the wild-type (A) and mutant type (G) alleles at position 6647 of the *NIPBL* gene in all the tested samples, demonstrating the absence of somatic mosaicism.

Furthermore, in the molecular context, the biallelic expression of *NIPBL* transcripts that contain exon 39 has been confirmed in all analyzed tissues. These results support the hypothesis of a dominant-negative effect or loss of function as the pathological mechanism of this *NIPBL* missense mutation.

The missense mutation p.(Tyr2216Cys) affects to the evolutionarily conserved residue Tyr 2216, which was located in an internal site of the HEAT repeat domain of *NIPBL*. Local disorganization caused by the mutation of Tyr 2216 by Cys would lead to changes in protein function and in the putative interaction of *NIPBL* to its accompanying macromolecules [Pié et al., 2010]. Classically, *NIPBL* missense mutations have been associated with a milder phenotype without any major limb malformations, contrary to nonsense or frameshift mutations, which are usually found in patients with major limb reduction defects [Oliveira et al., 2010]. However, among more than 250 mutations previously reported in the *NIPBL* gene, there are some exceptional cases of missense mutations mapped to the HEAT repeat elements, associated with severe limb reduction defects (reviewed in Pié et al., 2010) [Pié et al., 2010]; along with our case [Pié et al., 2010; Schoumans et al., 2007; Tonkin et al., 2004].

To the best of our knowledge, this is the first patient with CdLS who has severe unilateral upper and lower reduction defects. This case expands the spectrum of the limb anomalies related to CdLS, although this finding could be due to a random event. Finally, this case underscores the importance of assessment of multiple body tissue samples in patients with the clinical diagnosis of CdLS in order to rule out the possibility of somatic mosaicism.

Consent

The manuscript was written with the approval of Clinical Research Ethics Committee of Aragón, Spain. Written informed consent was obtained from the patient's parents for publication of this case report and any accompanying images.

Competing interests

The authors declare that they have no competing interests.

Acknowledgments

We sincerely thank the patient's family for participating in this study. This study was funded by grants from: The Spanish Ministry of Health – Fondo de Investigación Sanitaria (FIS) (Ref.#PI12/01318), the Diputación General de Aragón (Grupo Consolidado B20), the European Social Fund (Construyendo Europa desde Aragón), the Spanish Ministry of Economy and Competitiveness (Refs.# IPT2011-0964-900000 and # SAF2011-13156-E, to P.G-P) and the Fundació La Marató de TV3 (Exp. 101030 to E.Q). M.E.T-R is the recipient of a fellowship from University of Zaragoza (Ref.# PIF-UZ_2009-BIO-02). MCG-H, MH-M, MET-R, BP, FJR and JP are members of “Grupo Clínico asociado al CIBER-ER” at the University of Zaragoza Medical School and Hospital Clínico Universitario “Lozano Blesa”.

Appendix A. Supplementary data

Supplementary data related to this article can be found at <http://dx.doi.org/10.1016/j.ejmg.2014.05.006>.

References

- Ahmed AA, Imrie S, Duncan R, Tolmie J. Roberts syndrome: facial dysmorphology in a mildly affected case. *Clin Dysmorphol* 2009;18:236–7.
- Barboni C, Cereda A, Mariani M, Gervasini C, Ajmone P, Biondi A, et al. A new report of Cornelia de Lange syndrome associated with split hand and feet. *Am J Med Genet A* 2012;158A:2953–5.
- Bhuiyan ZA, Klein M, Hammond P, van Haeringen A, Mannens MM, Van Berckelaer-Onnes I, et al. Genotype-phenotype correlations of 39 patients with Cornelia de Lange syndrome: the Dutch experience. *J Med Genet* 2006;43:568–75.

- Deardorff MA, Kaur M, Yaeger D, Rampuria A, Korolev S, Pie J, et al. Mutations in cohesin complex members SMC3 and SMC1A cause a mild variant of Cornelia de Lange syndrome with predominant mental retardation. *Am J Hum Genet* 2007;80:485–94.
- Deardorff MA, Wilde JJ, Albrecht M, Dickinson E, Tennstedt S, Braunholz D, et al. RAD21 mutations cause a human cohesinopathy. *Am J Hum Genet* 2012;90:1014–27.
- Deardorff MA, Bando M, Nakato R, Watrin E, Itoh T, Minamino M, et al. HDAC8 mutations in Cornelia de Lange syndrome affect the cohesin acetylation cycle. *Nature* 2012;489:313–7.
- Dogan DG, Dogan M, Aslan M, Karabiber H. Bilateral split feet: a new finding in Cornelia de Lange syndrome. *Genet Couns* 2010;21:221–4.
- Gillis LA, McCallum J, Kaur M, DeScipio C, Yaeger D, Mariani A, et al. NIPBL mutational analysis in 120 individuals with Cornelia de Lange syndrome and evaluation of genotype-phenotype correlations. *Am J Hum Genet* 2004;75:610–23.
- Huisman S, Redeker E, Maas S, Mannens MM, Hennekam R. High rate of mosaicism in individuals with Cornelia de Lange syndrome. *J Med Genet* 2013 May;50(5):339–44. <http://dx.doi.org/10.1136/jmedgenet-2012-101477>.
- Kline AD, Krantz ID, Sommer A, Kliwer M, Jackson LG, FitzPatrick DR, et al. Cornelia de Lange syndrome: clinical review, diagnostic and scoring systems, and anticipatory guidance. *Am J Med Genet Part A* 2007;143A:1287–96.
- Krantz ID, McCallum J, DeScipio C, Kaur M, Gillis LA, Yaeger D, et al. Cornelia de Lange syndrome is caused by mutations in NIPBL, the human homolog of *Drosophila melanogaster* Nipped-B. *Nat Genet* 2004;36:631–5.
- Liu J, Krantz ID. Cornelia de Lange syndrome, cohesin, and beyond. *Clin Genet* 2009;76:303–14.
- Musio A, Selicorni A, Focarelli ML, Gervasini C, Milani D, Russo S, et al. X-linked Cornelia de Lange syndrome owing to SMC1L1 mutations. *Nat Genet* 2006;38:528–30.
- Oliveira J, Dias C, Redeker E, Costa E, Silva J, Reis Lima M, et al. Development of NIPBL locus-specific database using LOVD: from novel mutations to further genotype-phenotype correlations in Cornelia de Lange Syndrome. *Hum Mutat* 2010;31:1216–22.
- Petit F, Andrieux J, Demeer B, Collet LM, Copin H, Boudry-Labis E, et al. Split-hand/foot malformation with long-bone deficiency and BHLHA9 duplication: two cases and expansion of the phenotype to radial agenesis. *Eur J Med Genet* 2013;56:88–92.
- Pfeiffer RA, Correll J. Hemimelia in Brachmann-de Lange syndrome (BDLS): a patient with severe deficiency of the upper and lower limbs. *Am J Med Genet* 1993;47:1014–7.
- Pié J, Gil-Rodríguez MC, Ciero M, López-Viñas E, Ribate MP, Arnedo M, et al. Mutations and variants in the cohesion factor genes NIPBL, SMC1A, and SMC3 in a cohort of 30 unrelated patients with Cornelia de Lange syndrome. *Am J Med Genet A* 2010;152A:924–9.
- Roposch A, Bhaskar AR, Lee F, Adedapo S, Mousny M, Alman BA. Orthopaedic manifestations of Brachmann-de Lange syndrome: a report of 34 patients. *J Pediatr Orthop B* 2004;13:118–22.
- Schoumans J, Wincent J, Barbaro M, Djureinovic T, Maguire P, Forsberg L, et al. Comprehensive mutational analysis of a cohort of Swedish Cornelia de Lange syndrome patients. *Eur J Hum Genet* 2007;15:143–9.
- Selicorni A, Russo S, Gervasini C, Castronovo P, Milani D, Cavalleri F, et al. Clinical score of 62 Italian patients with Cornelia de Lange syndrome and correlations with the presence and type of NIPBL mutation. *Clin Genet* 2007;72:98–108.
- Tonkin ET, Wang TJ, Lisgo S, Bamshad MJ, Strachan T. NIPBL, encoding a homolog of fungal Scc2-type sister chromatid cohesion proteins and fly Nipped-B, is mutated in Cornelia de Lange syndrome. *Nat Genet* 2004;36:636–41.
- Yousoufian H, Pyeritz RE. Mechanisms and consequences of somatic mosaicism in humans. *Nat Rev Genet* 2002;3:748–58.